

RAPORTUL ȘTIINȚIFIC ȘI TEHNIC (RST)

Dezvoltarea unor biocatalizatori noi pentru obtinerea economica a unor sintoni chirali

Programul: Parteneriate in domenii prioritare PN-II-PT-PCCA-2011-3.1-1268

Acronim proiect: SYNBIOCAT

Contract nr: 124/2012

ETAPA 2016

APLICAȚII ALE BIOCATALIZATORILOR OBȚINUȚI

Având în vedere faptul că rezultatele experimentale incluse în această etapă a proiectului au constituit subiectele unor lucrări publicate sau acceptate spre publicare în reviste cotate ISI, respectiv au fost diseminate la conferințe internaționale. raportul va fi redactat în limba engleză, respectând informațiile originale din articolele menționate.

CONTENT

I. BIOTRANSFORMATION OF PYRIDINE IN A BIOREACTOR WITH IMMOBILIZED BIOCATALYSTS	2
1.1 General objectives - project stage abstract	2
1.2 Introduction	2
1.3 Stationary basket bioreactor with immobilized biocatalysts and operating conditions	3
1.4 Mathematical models for external and internal diffusion of pyridine	4
1.5 Diffusional analysis of pyridine biotransformation with immobilized biocatalysts	5
1.6 Selected references on part I	12
II. PREPARATION OF OPTICALLY ACTIVE IBUPROFEN USING A TWO STEPS INTERCONNECTED LIPASE CATALYZED KINETIC RESOLUTION SYSTEM	13
2.1 LIPASE-CATALYZED ESTERIFICATION OF THE IBUPROFEN	15
2.2 LIPASE-CATALYZED HYDROLYSIS OF IBUPROFEN ESTERS	16
2.3 ENANTIOSELECTIVE ALCOHOLYSIS OF RACEMIC IBUPROFEN ESTERS	16
2.4 EXPERIMENTAL SECTION	17
2.5 SELECTED LITERATURE ON PART II	19
III. DISEMINAREA REZULTATELOR CERCETĂRII AFERENTE ETAPEI ANULUI 2016	20

I. BIOTRANSFORMATION OF PYRIDINE IN A BIOREACTOR WITH IMMOBILIZED BIOCATALYSTS

1.1. GENERAL OBJECTIVES – PROJECT STAGE ABSTRACT

The researches included in this stage of the project have been focused on the pyridine biotransformation rate in a bioreactor with stationary basket bed of immobilized *Bacillus spp.* cells with various biocatalyst diameters and thicknesses of basket bed, considering the adapted Haldane kinetic model for substrate inhibition.

Due to the very low values of pyridine mass flow inside the biocatalyst particles, the extent of “biological inactive region” has been quantified, being located near the particles centre. This region was extended up to 38.5% from the overall volume of each studied size of the biocatalysts, being increased at higher biocatalyst size and basket bed width.

The cumulated analysis of the influences of the studied factors allowed concluding that the optimum diameter of biocatalysts is 3 mm.

1.2. INTRODUCTION

Pyridine is one of the most encountered and, implicitly, important pollutant from the N-heterocyclic compounds class. Although it can be naturally produced in the environment by metabolic pathways of various organisms, the main sources of pyridine are the chemical and related industries (dyes and solvents, pharmaceutical, food, adhesives and resins, oil and coal), as well as the use of pesticides and herbicides in agriculture (Pandoley et al. 2006; Li et al. 2009; Lian et al. 2010). Pyridine is known as a very toxic and rather persistent pollutant in environment compound, which affects sever the human and organisms health, being irritant, teratogenic, and carcinogenic.

The physical and chemical methods tested for treatment of wastewaters containing pyridine, namely adsorption on various natural or synthetic materials, oxidation and Fenton oxidation, electrochemical and ultrasonical methods (Bludau et al. 1998; Sabah and Celik, 2002; Mohan et al. 2005; Lataye et al. 2006; Gupta et al. 2007; Subbaramaiah et al. 2013; Pandoley et al. 2011; Elsayed, 2014) require important materials and energy consumption and offer rather low productivity (Pandoley et al. 2006; Lian et al. 2010).

Although the heterocyclic structure of pyridine does not make it a proper substrate for microbial consumption, the biological methods of pyridine removal from wastewaters became the most attractive alternative, because several species of microorganisms proved efficient affinity and activity for this compound or its derivatives biotransformation under anaerobic or aerobic conditions (*Azoarcus spp.*, *Arthrobacter spp.*, *Bacillus spp.*, *Brevibacterium spp.*, *Corynebacterium spp.*, *Lysinibacillus spp.*, *Micrococcus spp.*, *Nocardia spp.*, *Nocardioides spp.*, *Paracoccus spp.*, *Pimelobacter spp.*, *Pseudomonas spp.*, *Rhizobium spp.*, *Rhodococcus spp.*, *Shinella spp.*, *Shewanella spp.*, *Streptomyces spp.*) (Rhee et al. 1996; Pandoley et al. 2006; Mathur et al. 2008; Bai et al. 2009; Li et al. 2009; Lian et al. 2010; Yao et al. 2010; Shen et al. 2014).

The anaerobic biotransformation of pyridine occurs either by heterocycle reduction or hydroxylation, while the aerobic process is based on the successive steps of hydroxylation and heterocycle dioxygenolytic cleavage. According to the microorganisms metabolic pathway, the intermediate or final products are succinate or glutarate semialdehyde, succinate or glutarate, succinic or glutaric acid, formamide or ammonia (Rhee et al. 1997; Pandoley et al. 2006; Bai et al. 2008; Mathur et al. 2008).

Most of the biological treatments for wastewaters containing pyridine have been carried out using free cells of microorganisms, isolated as separate strain or in complex mixed cultures (activated sludge). The biotransformation efficiency, related to productivity and costs, could be improved by using immobilized microorganisms. In numerous cases, the immobilized microbial cells posses an increased thermal, chemical, and to the shear forces resistance, diminish or avoid the substrate inhibition processes, can be easier recovery without washing-out, and can be reused for many biosynthesis cycles (Galaction et al. 2012). Moreover, considering the particularities of the

wastewaters as growth medium for microorganisms, the immobilized cells are more resistant against the toxins, parasites or predators attacks (Lian et al. 2010).

Generally, the bioreactors with immobilized cells or enzymes use mobile bed (stirred or pneumatic bioreactors), packed bed (column bioreactors), or other configuration beds (membrane bioreactors, bioreactors with fluidization) (Caçcaval et al. 2012).

Although the bioreactors with fixed bed of biocatalysts are widely preferred, they have some major disadvantages. The flow inside the bed is laminar, thus leading to low rates of mass and heat transfer and inducing the back-mixing or reverse flow phenomenon. On the other hand, the solid particles from effluent can clog the biocatalyst bed, thus leading both to the reducing of the flow rate inside the bed, and to the biocatalysts inactivation. Another important undesirable phenomenon is the formation of the preferential flow channels inside the bed at the beginning of the feed with medium or during the bioreactor working. The formation of these channels lead to the deviation from the plug flow and the inefficient conversion of substrate.

The basket bed of immobilized biocatalysts represents a new configuration derived from the packed bed one, being designed as a cylindrical or conic annular bed, which is immobile or rotary around the stirrer (Sheelu et al. 2008; Caçcaval et al. 2012; Galaction et al. 2012). This biocatalysts bed configuration allows accelerating the flow velocity inside the bed and, consequently, the mass and heat transfer rates, avoids the reverse flow, clogging, and formation of the preferential flow channels specific to the packed bed column, as well as the flooding or deposition, and the mechanical disruption of the biocatalysts particles, phenomena induced in the mobile bed bioreactors. The complexity of medium hydrodynamics is the result of the combination between the perfect mixing around the basket bed and the plug flow inside it.

In this context, these experiments are dedicated to the investigation of the pyridine biotransformation by immobilized *Bacillus spp.* cells in a stationary basket bioreactor. In this purpose, considering that the bacterial process occurs under substrate inhibition restriction, the roles of external and internal diffusions of pyridine on its concentration profile in the outer region and inside the immobilized cells particle, as well as on its biotransformation rate have been analyzed. The influences of the studied factors have been included in mathematical models describing the pyridine concentrations and mass flows around and inside the biocatalyst particle, and, finally, have been quantified as the effectiveness factor corresponding to the relative rate of biotransformation process using immobilized *Bacillus spp.* cells compared to that of the process with free bacterial cells.

1. 3. STATIONARY BASKET BIOREACTOR WITH IMMOBILIZED BIOCATALYSTS AND OPERATIVE CONDITIONS

The experiments have carried out in 10 l (8 l working volume) modified laboratory stirred bioreactor Fermac 310/60 (Electrolab), provided with a static cylindrical bed of basket type, placed around the impeller shaft at 100 mm from the bioreactor bottom (Galaction et al. 2012). The basket consists on plastic mesh, its geometrical characteristics being: inner diameter 100 mm, height 100 mm, thickness 10 mm. The impellers configuration and position correspond to those found to be optimum in the previous works (Caçcaval et al. 2012). Therefore, the mixing system was configured as two Rushton turbines, one being placed outside the basket over its superior extremity, while the other one inside the basket close to its inferior extremity. The impeller rotation speed was maintained at the constant value of 300 rpm.

The basket was filled with immobilized biocatalysts consisting on mixture of *Bacillus spp.* (*Bacillus subtilis*, *Bacillus megaterium*, *Bacillus licheniformis* and *Bacillus ortoliquefaciens* in equal ratios) immobilized by inclusion into alginate particles (William and Munnecke, 1981). In this purpose, 7.5 g d.w. bacterial mixture were mixed with 100 ml of 5% aqueous solution of sodium alginate, this suspension being dripped at constant pressure through a capillary into a solution of 0.2% CaCl₂. Because capillaries with four different diameters have been used, the immobilized bacterial cells particles resulted with the following diameters: 2.4, 3.0, 3.6, and 4.2 mm. The working size of the biocatalyst particles corresponds to the following volumetric fractions inside the basket bed: 0.82 for biocatalysts particle with 2.4 mm diameter, 0.79 for biocatalysts

particles with 3.0 mm diameter, 0.74 for biocatalysts particles with 3.6 mm diameter, and 0.70 for the largest biocatalyst particles.

The composition of one liter of medium containing pyridine respects that previously used for this bacteria type: pyridine 0.5 g, KH_2PO_4 0.9 g, $\text{Na}_2\text{HPO}_4 \cdot 2\text{H}_2\text{O}$ 2.3 g, KNO_3 3 g, $(\text{NH}_4)_2\text{SO}_4$ 1.9 g, $\text{MgSO}_4 \cdot 7\text{H}_2\text{O}$ 0.5 g, $\text{CaCl}_2 \cdot 2\text{H}_2\text{O}$ 0.5 g, $\text{FeSO}_4 \cdot 7\text{H}_2\text{O}$ 0.02 g, $\text{MnSO}_4 \cdot 7\text{H}_2\text{O}$ $8 \cdot 10^{-4}$ g, $\text{ZnSO}_4 \cdot 7\text{H}_2\text{O}$ $4 \cdot 10^{-4}$ g, $\text{Na}_2\text{MoO}_4 \cdot 2\text{H}_2\text{O}$ $1 \cdot 10^{-3}$ g, $\text{CoCl}_2 \cdot 6\text{H}_2\text{O}$ $8 \cdot 10^{-4}$ g (Mathur et al. 2008). The biotransformation process temperature was maintained at 30°C. The end of the process has been assumed when the pyridine concentration became 0 or reached a constant level for 6 h.

The experimental values of pyridine mass transfer rate in the outer region of biocatalyst particle have been calculated by means of the variations of its concentrations in the medium bulk volume and at biocatalysts particle surface during the fermentation. The pyridine concentration has been measured by high performance liquid chromatography technique (HPLC) with a using a C18 column (Agilent HCC18, 4.6 mm diameter, 250 mm length, 5 μm pores diameter), provided with UV detector at 270 nm. The mobile phase was a solution methanol:water in a volumetric ratio of 60:40. Its flow rate was 0.6 ml/min.

The values of pyridine concentration or mass transfer inside the immobilized *Bacillus spp.* cells particles have been calculated using the proposed mathematical models.

Each experiment was in duplicate or triplicate, the average value of the analyzed parameters being considered. The maximum experimental deviation was 7.87%.

1.4. MATHEMATICAL MODELS FOR EXTERNAL AND INTERNAL DIFFUSION OF PYRIDINE

The immobilization of cells or enzymes inside of an inert support leads to the appearance of the substrate or product internal diffusion, which could affects strongly the rate of biochemical reactions. In the studied system, the pyridine has to migrate to the *Bacillus spp.* cells through non-linear channels, its internal diffusion being described by the effective diffusivity.

The values of pyridine concentrations at the immobilized cells particle surface and inside this particle can be obtained using its mass balance related to a single biocatalyst particle. In this purpose, the following assumptions have been considered:

- the kinetics of pyridine consumption is subject of substrate inhibitory effect, being described by the Haldane model adapted to the immobilized biocatalysts (Shen et al. 2014):

$$r = \frac{V \cdot C_C \cdot C_S}{K'_M + C_S + \frac{C_S^2}{K_I}} \quad (1)$$

- the immobilized cells particle is spherical;
- the distribution of bacterial cells inside the particle is uniform;
- no interactions occur between the support and the reactants or products;
- the internal diffusion respects the Fick law and can be described by effective diffusivity.

The expression for the mass balance of pyridine related to the biocatalyst particle is obtained by means of Bird equation (Bird et al. 1960):

$$\frac{dC_S}{dt} = D_{Se} \cdot \left[\frac{1}{r^2} \cdot \frac{d}{dr} \left(r^2 \cdot \frac{dC_S}{dr} \right) \right] - \frac{V \cdot C_C \cdot C_S}{K'_M + C_S + \frac{C_S^2}{K_I}} \quad (2)$$

Assuming the steady-state conditions for pyridine diffusion and consumption by cells, the equation (2) becomes:

$$\frac{d^2 C_{SP}}{dr^2} + \frac{2}{r} \cdot \frac{dC_{SP}}{dr} = \frac{1}{D_{Se}} \cdot \frac{V \cdot C_C \cdot C_{SP}}{K'_M + C_{SP} + \frac{C_{SP}^2}{K_I}} \quad (3)$$

The solutions of equation (3) can be found considering the following boundary limits:

$$1) \quad r = 0 \text{ (at particle centre), } \frac{dC_{SP}}{dr} = 0 \quad (4)$$

$$2) \quad r = R_p \text{ (at particle surface), } -D_{Se} \cdot \frac{dC_{SP}}{dr} = k_L \cdot (C_{SL} - C_{Si})$$

The solutions of equation (3) was calculated by Prelle-Singer method for finding the first integrals, the closed form solutions of first order differential equations, and the Kovacic results on second order linear ordinary differential equations as well (Prelle and Singer, 1983). Therefore, the profiles of pyridine concentration inside the immobilized *Bacillus spp.* cells particles, C_{SP} , and at the particles surface, C_{Si} , represent the two solutions of equation (3):

$$C_{SP} = \frac{R_p \cdot \sinh(3\phi \cdot r)}{r \cdot \cosh(3\phi \cdot R_p)} \cdot \frac{(C_{SL} - C_{Si}) \cdot B_i \cdot k_L \cdot V \cdot C_C}{3\phi \cdot B_i \cdot D_{Se} - k_L \cdot \tanh(3\phi \cdot R_p) + K_I} \quad (5)$$

$$C_{Si} = \frac{\tanh(3\phi \cdot R_p) \cdot C_{SL} \cdot B_i \cdot k_L \cdot V \cdot C_C}{3\phi \cdot B_i \cdot D_{Se} + k_L \cdot \tanh(3\phi \cdot R_p) \cdot [B_i \cdot k_L \cdot V \cdot C_C - 1] + K_I} \quad (6)$$

The expressions (4) and (5) include two parameters specific to the diffusional processes coupled with chemical or biochemical reactions, namely the Thiele modulus, ϕ , and Biot number, Bi . The Thiele modulus represents the measure of the magnitude of internal diffusion effect on the substrate consumption rate (Caçcaval et al. 2012). The Thiele modulus specific to the bacterial consumption of pyridine is defined by the expression:

$$\phi = \frac{R_p}{3} \cdot \sqrt{\frac{V}{K_M \cdot D_{Se}}} \quad (7)$$

The Biot number quantifies the relative importance of the external and internal diffusion processes, being calculated as the ratio between the resistance to the diffusion in the boundary layer surrounding the biocatalyst particle and that related to the internal diffusion (Caçcaval et al. 2012):

$$Bi = \frac{k_L \cdot R_p}{D_{Se}} \quad (8)$$

The external and internal mass transfer rates of pyridine are calculated by means of concentrations values in the liquid bulk and inside the immobilized cells particle. In this context, the substrate mass flow from the liquid phase to the surface of the solid particle of biocatalyst is described by the following relationship:

$$n_L = k_L \cdot (C_{SL} - C_{Si}) \quad (9)$$

The mass transfer coefficient related to the boundary layer at the particle surface, k_L , is calculated with the expression considered for the biocatalysts disposed in packed bed conformation (Perry and Chilton, 1973):

$$k_L = 5.7 \cdot \frac{(1-\phi)^{0.78} \cdot \eta_L^{0.11} \cdot v_s^{0.22} \cdot D_{SL}^{2/3}}{\rho_L^{0.11} \cdot d_p^{0.78}} \quad (10)$$

For determining the liquid phase superficial velocity, the radial flow rate of Rushton turbine is used, assuming that the liquid phase flows from the basket bed inner surface to its outer one (Galaction et al. 2012). In this case, because the value of ratio between impeller diameter and that of bioreactor is varied between the limits 0.2 - 0.4, the following relationship is adequate for calculating the velocity of liquid flow through the cylindrical section of the basket (Harnby et al. 1997):

$$v_s = 0.75 \cdot \frac{N \cdot d^3}{(1-\phi) \cdot \pi \cdot R_C \cdot H_C} \quad (11)$$

For describing mathematically the internal mass flow of pyridine, the Fick law:

$$n_p = -D_{Se} \cdot \frac{dC_{SP}}{dr} \quad (12)$$

is combined with expression (5), resulting:

$$n_p = -D_{Se} \cdot \frac{R_p \cdot (C_{SL} - C_{Si}) \cdot B_i \cdot k_L \cdot V \cdot C_C \cdot [r \cdot \phi \cdot \cosh(3\phi \cdot R_p) - \sinh(3\phi \cdot R_p)]}{r^2 \cdot \cosh(3\phi \cdot R_p) \cdot [3\phi \cdot B_i \cdot D_{Se} - k_L \cdot \tanh(3\phi \cdot R_p) + K_I]} \quad (13)$$

The negative effect of internal diffusion on the rate of pyridine consumption by the *Bacillus spp.* cells inside the biocatalyst particle can be quantified by the effectiveness factor λ , defined as

the ratio between the rate of the biotransformation process in heterogeneous system and that corresponding to the homogeneous one. Assuming that pyridine diffusion and biotransformation occur in steady-state regime, the rate of its consumption inside the solid particle is equal to its internal mass transfer rate. Consequently, the relationship for calculating the factor λ given below is adequate for the studied biotransformation system:

$$\lambda = \frac{4\pi \cdot R_p^2 \cdot D_{Se} \cdot \left. \frac{dC_{SP}}{dr} \right|_{r=R_p}}{\frac{4}{3}\pi \cdot R_p^3 \cdot \frac{V \cdot C_C \cdot C_{Si}}{K'_M + C_{Si} + \frac{C_{Si}^2}{K_I}}} \quad (14)$$

By replacing the pyridine concentration inside the biocatalyst particle from equation (5) in the expression (14), the relationship for calculating factor λ becomes:

$$\lambda = \frac{3D_{Se} \cdot (C_{SL} - C_{Si}) \cdot \left(K'_M + C_{Si} + \frac{C_{Si}^2}{K_I} \right) \cdot B_i \cdot k_L \cdot \left[R_p \cdot \phi \cdot \cosh(3\phi \cdot R_p) - \sinh(3\phi \cdot R_p) \right]}{R_p^2 \cdot C_{Si} \cdot \cosh(3\phi \cdot R_p) \cdot \left[3\phi \cdot B_i \cdot D_{Se} - k_L \cdot \tanh(3\phi \cdot R_p) + K_I \right]} \quad (15)$$

The values of the parameters considered for calculating the external and internal concentrations and, respectively, mass flows of pyridine, as well as the effectiveness factor, have been previously determined for similar conditions, being given in Table 1.

NOTATIONS

- C_S - pyridine concentration (mol/m³)
- C_{Si} - pyridine concentration at biocatalyst particle surface (mol/m³)
- C_{SL} - pyridine concentration in liquid phase (mol/m³)
- C_{SP} - pyridine concentration inside the biocatalyst particle (mol/m³)
- C_{SPo} - pyridine concentration at the biocatalyst particle centre (mol/m³)
- d - impeller diameter (m)
- d_p - biocatalyst particle diameter (m)
- D_{Se} - pyridine effective diffusivity (m²/s)
- D_{SL} - pyridine liquid phase diffusivity (m²/s)
- H_C - basket bed height (m)
- k_L - liquid phase mass transfer coefficient of Pyridine (m/s)
- K_I - pyridine inhibition constant (mol/m³)
- K_M - apparent Michaelis-Menten constant (mol/m³)
- N - rotation speed (s⁻¹)
- n_L - pyridine external mass flow (mol/m².s)
- n_p - pyridine internal mass flow (mol/m².s)
- R_C - basket bed radius (m)
- R_p - biocatalyst particle radius (m)
- v_S - liquid superficial velocity (m/s)
- V - maximum biotransformation reaction rate (s⁻¹)

Greek symbols

- ϕ - volumetric fraction of biocatalyst particles (-)
- η_L - liquid phase viscosity (N/m².s)
- ρ_L - liquid phase density (kg/m³)
- λ - effectiveness factor (-)

1.5. DIFFUSIONAL ANALYSIS OF PYRIDINE BIOTRANSFORMATION WITH IMMOBILIZED BIOCATALYSTS

Assuming that the radial flow of liquid phase is constant, Fig. 1 indicates that the values of liquid superficial velocity reached inside the packed bed are superior to those related to the outer region of the basket, for all considered diameter of the biocatalysts particles.

This variation is the consequence of the reduction of the area of flow section. On the other hand, the superficial velocity of the liquid phase through the basket bed decreases radially, due to the increase of the area of the cylindrical flow section.

The superficial velocity of the liquid phase decreases from the smallest to the largest particles of immobilized *Bacillus spp.* cells, owing to the increasing of the void fraction of the packed bed. Consequently, regardless of the position inside the basket bed, the superficial velocity

corresponding to the biocatalyst particles with 2.4 mm diameter is for about 1.7 times higher than that recorded for the biocatalyst particles having the diameter of 4.2 mm. This difference suggests an increased turbulence inside the biocatalyst bed for the smallest particles.

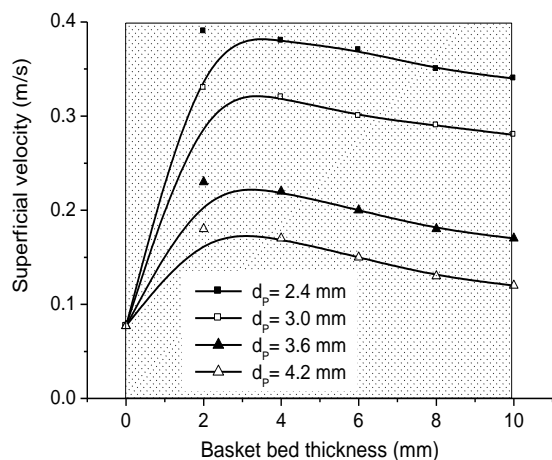


Fig. 1.1. Variation of liquid phase superficial velocity inside the basket bed.

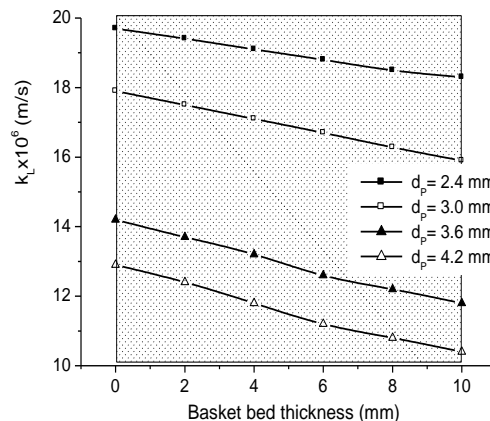


Fig. 1.2. Variation of pyridine external mass transfer coefficient inside the basket bed

Obviously, the variation of pyridine mass transfer coefficient in the liquid boundary layer at the particle surface is directly depended on the variation of the superficial velocity of liquid phase. Therefore, according to Fig. 1.2, the external mass transfer coefficient of pyridine is reduced with about 8 to 25% from the inner to the outer surface of the basket bed simultaneously with the diminution of turbulence (the effect becomes more important by increasing the size of the biocatalyst particles).

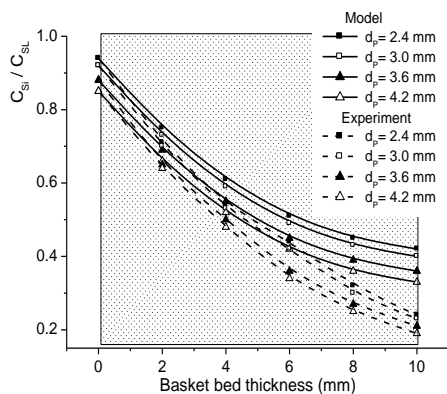


Fig. 1.3. Variation of ratio C_{Si}/C_{SL} inside the basket bed.

This radial reduction of the concentrations ratio is the result of the cumulated phenomena of the decrease of transfer rate through the liquid boundary layer and of pyridine biotransformation by the bacterial cells, both acting mainly on the ratio numerator.

Analyzing the experimental data plotted in Fig. 3, it can be observed deviations from the ratio values calculated by means of equation (6). For all considered diameters of immobilized bacterial cells, the ratio between the experimental values of pyridine concentrations at the biocatalyst particle surface and in the liquid phase inside the basket bed is inferior to that obtained using the calculated value of pyridine superficial concentration. This difference becomes more pronounced by reducing the biocatalyst particle size and is amplified by increasing the bed thickness over 4 mm. The deviations of the experimental ratios from the calculated ones could be the result of the radial augmentation of resistance to pyridine diffusion inside the basket bed from

However, compared to the pyridine biotransformation in a bioreactor with mobile bed of identical particles of immobilized bacterial cells (Caçcaval et al. 2015), for the basket conformation of the biocatalyst bed the rate of substrate external mass transfer through the liquid boundary layer is lowered for about 2.5 - 5.5 times, this difference being amplified by enlarging the particle diameter and width of biocatalysts basket bed.

Regardless of the particle size of immobilized *Bacillus spp.* cells, the variation of ratio between the calculated pyridine concentrations at the biocatalyst particle surface and in the liquid phase from the inside of the bed decreases from the inner surface of the basket bed to the outer one (Fig. 1.3).

its inner surface to the outer one cumulated with the enhancement of biotransformation rate, due to the radial increase of pyridine residence time inside the basket bed.

Because the smaller particles of immobilized bacterial cells generate smaller void fractions of the basket bed, for the particles with 2.4 and 3 mm diameter the resistance to the pyridine diffusion inside the bed is increased and, consequently, the deviations from the model is more significant.

For calculating the pyridine mass flow through the liquid boundary layer surrounding the immobilized cells particle the equation (9) and the above data have been used. Therefore, the radial variation of external mass flow inside the basket bed was plotted in Fig. 1.4 for the four biocatalyst sizes and considering both the experimental and calculated values of pyridine concentration at the biocatalyst particle surface.

From Fig. 1.4 it can be seen that the pyridine mass flow varies radially inside the basket bed contrary to its mass transfer coefficient. This opposite influence of bed thickness suggests that the pyridine concentration gradient between the liquid phase and the particle surface controls its transfer through the liquid boundary layer surrounding the biocatalyst particles, the pyridine diffusivity exhibiting a less important influence. Moreover, by increasing the basket bed width, the biotransformation rate of pyridine is accelerated, this leading to the amplification of pyridine concentration gradient and, implicitly, to the increase of external mass transfer rate of this compound. For the basket bed thickness over 2 – 3 mm, the magnitude of this phenomenon becomes more important by reducing the size of the immobilized *Bacillus spp.* particles, due both to the increased turbulence inside the biocatalysts bed and to the superior rate of pyridine consumption, as the result of lower resistance to pyridine internal diffusion inside the smaller particles.

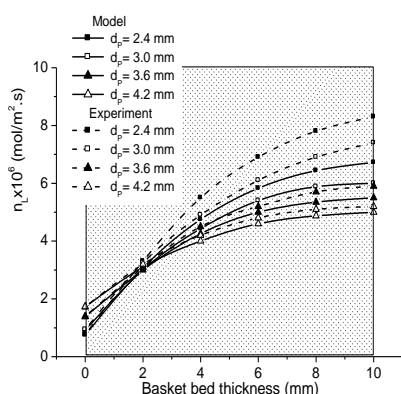


Fig. 1.4. Variation of pyridine external mass flow inside the basket bed.

As it was afore mentioned, the configuration of packed bed type hinders significantly the liquid phase circulation around the biocatalyst particles related to the mobile bed. In these circumstances, the pyridine external mass flow obtained for the basket bed is reduced between 1.5 and 6.7 times compared to a stirred bioreactor containing the same biocatalysts and respecting the same biotransformation process conditions (Caçcaval et al. 2015). For the above discussed reasons, the differences between the values of pyridine external mass flow corresponding to the mobile bed and, respectively, to the packed one with basket configuration is amplified by increasing the diameter of biocatalyst particles and radius of basket bed.

Due to this variation of ratio C_{SP}/C_{Si} , the pyridine concentration in the biocatalyst particle centre is significantly lower compared to its concentration at the particle surface, the difference between these two concentrations being enhanced by increasing the biocatalyst size. Therefore, in the centre of immobilized *Bacillus spp.* cells particles, the ratio C_{SP}/C_{Si} reaches 0.43 - 0.82, the superior values corresponding to the smallest biocatalysts. This result cumulated with the above

discussed one confirms the limiting role of the internal diffusion in the distribution of pyridine concentration inside the biocatalysts particles.

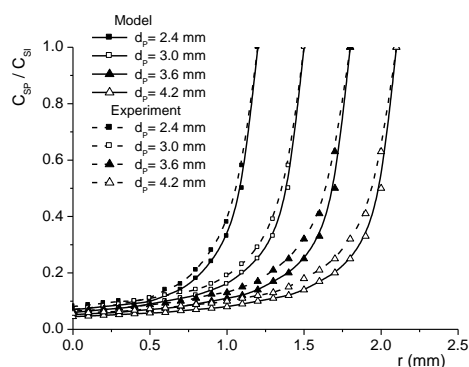


Fig. 1.5. Variation of ratio C_{SP}/C_{Si} with distance from the biocatalyst particle centre.

The percent from the biocatalyst particle radius related to the significant diminution of the two pyridine concentrations ratio decreases from 50% for particles with 2.4 mm diameter to 17% for the largest biocatalysts. The variations of ratio C_{SP}/C_{Si} plotted in Fig. 1.5 are similar both for the experimental values of C_{Si} or for those calculated with equation (6). However, although the model fits well with the experimental variations, it can be observed that the ratio values calculated by means of the experimental C_{Si} are higher. This deviation can be explained by supplementary reduction of C_{Si} in the real system compared to its theoretical variation, as it was suggested by Fig. 1.3.

The magnitude of the limitation induced by the resistance to the internal diffusion of pyridine is changed by increasing the basket bed thickness. Thus, the diffusion rate in the largest biocatalyst particles is affected mainly in the first half of basket bed thickness, the resistance to the pyridine diffusion becoming more important for the smallest biocatalysts for the basket bed width over 5 mm. This change in the relative importance of the internal diffusion resistance is the result of the cumulation with the effect of biotransformation process, which leads to an accelerated consumption of pyridine in the particles with lower size.

The internal mass flow of pyridine can be calculated by means of expression (13). The significant negative effect of internal diffusion on pyridine transfer rate is suggested by the reduction with four order size of its mass flow inside the biocatalyst particle compared to its mass flow in the liquid layer at the particle surface. Moreover, compared to the pyridine external mass flow, the internal rate of its mass transfer is reduced by increasing the basket bed width, due to the reduction of the substrate concentration gradient between the external and internal regions related to biocatalyst. In this context, the results indicate the direct correlation between the pyridine internal mass flow and its concentration inside the biocatalyst particle, because both parameters are significantly reduced from the surface to the centre of particle.

The presented radial variations of pyridine transfer rate inside the immobilized *Bacillus spp.* cells particles suggests that its internal mass flow could become very low or negligible near the centre of biocatalysts. Similar to other biological or enzymatic processes using immobilized cells or enzymes, the region placed near the biocatalyst centre could be considered as a “biological inactive region” (Caşcaval et al. 2012; Galaction et al. 2012). For quantifying the extent of this inactive region inside the biocatalyst particle, it was compared the values of pyridine internal mass flow with that of its effective diffusivity (Caşcaval et al. 2012; Galaction et al. 2012). Therefore, it can be assumed that the biological inactive region corresponds to the values of pyridine internal mass flow up to 10^{-10} mol/m².s.

As it can be observed from Fig. 1.7, the extent of biological inactive region depends on the biocatalyst particle size and position inside the basket bed, varying from 0% (for the biocatalyst

The pyridine concentration inside the particle of immobilized bacterial cells is strongly depended on its concentration at the particle surface. Therefore, the effect of internal diffusion could be described more accurately by considering the variation of the ratio between the pyridine concentration inside the biocatalyst and its superficial one with the particle radius. In this case, the experimental and calculated values of superficial concentration are also considered. According to Fig. 1.5, regardless of biocatalyst particle diameter or position inside the basket bed, the ratio C_{SP}/C_{Si} is strongly reduced in the region closed to the particle surface, this variation becoming considerably attenuated towards the biocatalyst centre.

particles with 2.4 mm diameter placed closed to the inner surface of the basket bed) to 38.5% from the overall volume of each biocatalyst particle (for the particles with 4.2 mm diameter placed near the outer surface of basket bed).

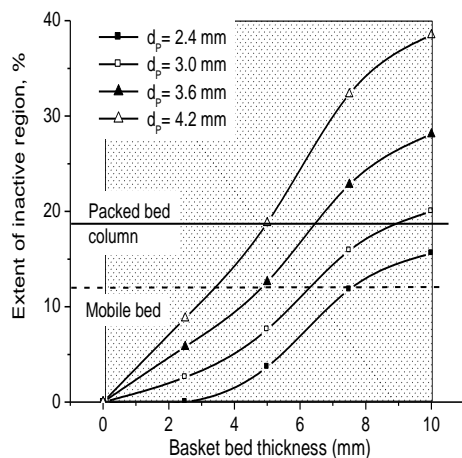


Fig. 1.7. Extent of biological inactive region inside the biocatalyst particle for different thickness of basket bed.

Compared to the mobile bed bioreactor, the thickness of the basket bed related to a lower extent of the inactive region induced in the basket bioreactor varies from 7 mm for the smallest biocatalyst particles to 3 mm for the largest ones, respectively.

According to those aforementioned, the solutions of equation (3) include the Biot number, Bi , and the Thiele modulus, ϕ . These two parameters quantify the effect induced by the internal diffusion of pyridine on its transfer process or on its biotransformation rate, respectively.

As can be seen from equation (7), Thiele modulus is specific for a certain diameter of immobilized *Bacillus spp.* cells particles, being not affected by the pyridine concentration or position inside the basket bed. In fact, the values of this parameter are the same as those calculated for the bioreactor with mobile bed ($\phi = 0.04$ for the biocatalysts with 2.4 mm diameter, $\phi = 0.05$ for the biocatalysts with 3 mm diameter, $\phi = 0.06$ for the biocatalysts with 3.6 mm diameter, $\phi = 0.07$ for the biocatalysts with 4.2 mm diameter). Obviously, the increase of modulus Thiele value from the smallest biocatalyst particles to the largest ones indicates the increase of the relative importance of limitation induced by pyridine diffusion compared to that related to its biotransformation process.

However, the highest Biot number corresponds to the particles having 3.0 mm diameter, probably due to the optimum equilibrium established at this size of biocatalyst between the rates of pyridine external, internal, and inside the basket bed diffusion. Taking into account this result and considering also those obtained for the bioreactor with mobile bed of immobilized *Bacillus spp.* cells (Caçcaval et al. 2015), it can be concluded that 3.0 mm represents the optimum diameter of the biocatalyst particles. Fig. 1.8 suggests that the relative magnitude of resistances to the pyridine diffusion in the liquid boundary layer surrounding the biocatalyst particle and, respectively, inside the biocatalyst, depends on the size and concentration of immobilized cells particles. In this context, regardless of the biocatalyst particles diameter, the Biot number is reduced radially from the inner surface of the basket bed to its outer one. Higher values of this number are reached for the smaller biocatalyst particles. These recorded variations are the result of the above discussed correlation between the pyridine external mass transfer rate and the basket bed width or particle size.

The comparison between the values of Biot number obtained for the four sizes of biocatalysts particles size averaged for the entire width of basket bed ($Bi = 75.2$ for the biocatalysts with 2.4 mm diameter, $Bi = 78$ for the biocatalysts with 3.0 mm diameter, $Bi = 72.2$ for the biocatalysts with 3.6 mm diameter, and $Bi = 69.7$ for the biocatalysts with 4.2 mm diameter) with those previously recorded for the mobile bed of immobilized *Bacillus spp.* cells with the same

By comparing the extent of the inactive region for three types of bioreactors containing different configurations of immobilized bacterial cells particles, it can be observed that the basket bioreactor is more efficient than the mobile bed bioreactor (Caçcaval et al. 2015) or packed bed column (Zaiat et al. 2000) for the basket bed thickness up to 3 mm, regardless of the biocatalyst size (Fig. 1.7). The increase of biocatalyst diameter cumulated with that of basket bed width leads to the reduction of the efficiency of basket bioreactor from the viewpoint of the extent of inactive region, effect that is more pronounced for the larger particles of biocatalysts. Therefore, for the biocatalysts with diameters of 2.4 and 3 mm, the basket bioreactor is more efficient than the packed bed column regardless of the thickness of basket bed (the considered packed bed column contained biocatalysts with 3 mm diameter (Zaiat et al. 2000)).

diameters ($Bi = 268.5$ for the biocatalysts with 2.4 mm diameter, $Bi = 328.3$ for the biocatalysts with 3.0 mm diameter, $Bi = 252.7$ for the biocatalysts with 3.6 mm diameter, and $Bi = 222.3$ for the biocatalysts with 4.2 mm diameter (Caçaval et al. 2015)) reveals that the Biot number for the basket bed is for about 3 - 4 times lower than that for the mobile bed bioreactor.

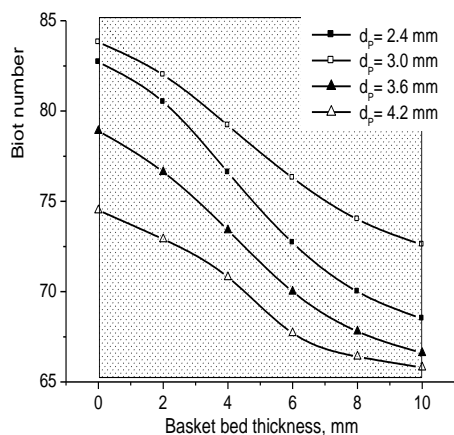


Fig. 1.8. Variation of Biot number inside the basket bed

This difference can be attributed to the reduction of pyridine mass transfer rate in the liquid boundary layer at the surface of biocatalysts from the basket bed, as the result of the turbulence decrease inside the packed bed compared to the mobile one and, implicitly, to the appearance of the supplementary resistance to the pyridine substrate diffusion inside the basket bed (this type of diffusional resistance is not encountered in the case of mobile bed).

As it was mentioned above, the effectiveness factor λ represents the measure of the reduction of biotransformation rate by immobilizing the *Bacillus spp.* cells in an inert support. The variation of factor λ towards the biocatalyst particle centre is plotted in Fig. 1.9.

Regardless of the biocatalyst size and position inside the basket bed, Fig. 1.9 indicates that the variation of effectiveness factor is considerably attenuated in the regions placed near the biocatalyst surface and centre. Because the pyridine concentration inside the particle near its surface is similar to pyridine concentration at particle surface, the values of λ are close to 1. The percentage of the distance from the particle surface to its centre corresponding to the reduction of λ from 1 to 0.95 varies from 10% to over 50%, being reduced by enlarging the biocatalyst particles and increasing the cylindrical bed width. The most extended region related to this slow variation of effectiveness factor was recorded for de biocatalyst with 3.0 mm diameter, for the above discussed reasons.

The factor λ varies slowly also in the central region of the particles. As can be seen from Fig. 1.6, this variation can be attributed to the constant low level of pyridine concentration near the centre. Being directly depended on the variation of pyridine concentration inside the immobilized *Bacillus spp.* cells particle, the thickness of the intermediary region corresponding to the significant reduction of λ from its value at the particle surface to that for the particle centre is increased by increasing the particles diameter and basket bed width.

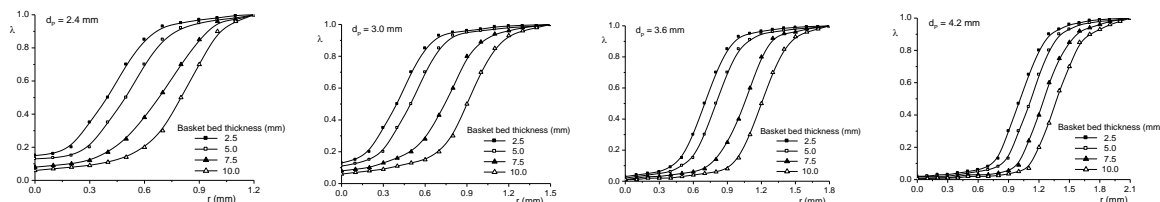
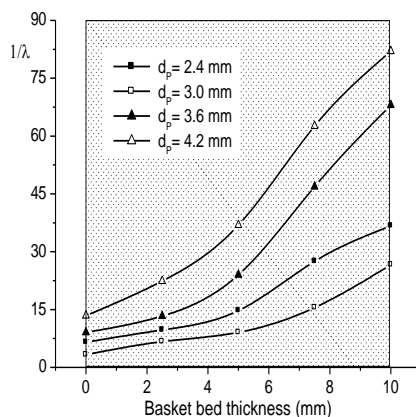


Fig. 1.9. Radial variation of effectiveness factor λ inside the biocatalyst particle.

On the basis of effectiveness factor values, it can be concluded that the rate of the pyridine biotransformation is reduced for $1/\lambda$ times by immobilizing *Bacillus spp.* cells compared to the system containing free bacterial cells. The magnitude of the reduction effect is directly correlated with the size of particles and their position inside the basket bed. Therefore, in the superficial region of the biocatalysts corresponding to $\lambda = 0.95 - 1$, the biotransformation rate is practically not affected by the immobilization of *Bacillus spp.* cells. From this viewpoint, the biocatalysts with diameter of 3 mm allow maintaining high biotransformation rate in the first 50% of distance from their surface to centre, while the largest biocatalysts only in the first 10%.

The most drastic decrease of pyridine biotransformation rate compared to the system with free *Bacillus spp.* cells is reached in the biocatalysts particles centre. Fig. 10 underlines that the increase of the basketed bed width leads to the amplification of this reduction effect. Therefore, depending on the biocatalyst size, at the outer surface of the cylindrical packed bed, the rate of pyridine biotransformation in the centre of biocatalyst becomes for 36 - 82 times lower than that for the homogeneous system (obviously, the reduction is more pronounced for the larger biocatalysts).



In the same time, Fig. 1.10 indicates that the effect of internal diffusion is less important for the biocatalysts having 3 mm diameter, result which confirms also that this size of immobilized *Bacillus spp.* cells particles represents the optimum one in the given experimental conditions.

In conclusion, the biotransformation of pyridine with immobilized *Bacillus spp.* cells in a bioreactor with stationary basket bed has been discussed in relation with the influences of its diffusion inside the biocatalyst particles on the rates of mass transfer and bacterial consumption. For underlining the role of biocatalysts bed characteristics, the results have been analyzed for four biocatalyst particle diameters, varying from 2.4 to 4.2 mm, and various positions inside the basket bed.

Fig. 1.10. Variation of parameter $1/\lambda$ calculated at the biocatalyst centre inside the basket bed

For calculating the pyridine concentrations at the surface of biocatalysts and inside them, the Haldane kinetic model for substrate inhibitory effect and adapted to the immobilized bacterial cells has been used. By means of the experimental and calculated concentrations of pyridine, its external and internal mass flows have been predicted. By comparing the external mass transfer rates corresponding to the basket bed with those recorded for mobile bed of the same biocatalysts, it was concluded that the former ones are for 1.5 - 6.7 times lower, difference which is amplified by increasing the diameter of biocatalyst particles and radius of basket bed.

The pyridine mass flow inside the immobilized *Bacillus spp.* cells particles is reduced for 10^4 times compared to its mass flow in the liquid phase surrounding these particles. In these circumstances, the internal mass flow could reach very low levels near the particles centre. The region inside the particles which corresponds to the rate of pyridine mass transfer below 10^{-10} mol/m².s was defined as “biological inactive region”. The extent of this region varies between 0 and 38.5% from the overall volume of each studied size of the biocatalysts, being increased by enlarging the biocatalyst particles and basket bed width.

The influence of internal diffusion of pyridine on its biotransformation rate has been analyzed also by means of the Bi number, Thiele modulus, and effectiveness factor λ . The increase of the biocatalyst size led to the reduction of Bi number, increase of Thiele modulus, and decrease of factor λ in the particle. The pyridine biotransformation rate decreased radially inside the basket bed from 5.6 to 7.5 times, the magnitude of this variation being amplified for larger particles of biocatalysts.

By analyzing the mentioned factors, it was concluded that the optimum diameter of immobilized *Bacillus spp.* cells particles is 3 mm, similar to the mobile bed of the same biocatalysts, due to the less important influence of external and internal diffusion of pyridine on its biotransformation rate by immobilized bacterial cells.

1. 6. SELECTED REFERENCES ON PART I

1. Bai Y, Sun Q, Zhao C, Wen D, Tang X (2008) Microbial degradation and metabolic pathway of pyridine by a *Paracoccus sp.* strain BW001. *Biodegradation* 19:915-926.
2. Bai Y, Sun Q, Zhao C, Wen D, Tang X (2009) Aerobic degradation of pyridine by a new bacterial strain, *Shinella zoogloeoides* BC026. *J Ind Microbiol Biotechnol* 36:1391-1400.
3. Bird RB, Stewart WE, Lightfoot EN (1960) *Transport Phenomena*. Wiley, New York
4. Bludau H, Karge HG, Niessen W (1998) Sorption kinetics and diffusion of pyridine in zeolites. *Micropor Mesopor Mater* 22:297-308.

5. Caşcaval D, Galaction AI, Blaga AC (2015) Biodegradation of pyridine in a bioreactor with mobile bed of immobilized *Bacillus spp.* cells. Chem Eng J accepted.
6. Caşcaval D, Turnea M, Galaction AI, Blaga AC (2012) 6-Aminopenicillanic acid production in stationary basket bioreactor with packed bed of immobilized penicillin amidase - Pyridine mass transfer and consumption rate under internal diffusion limitation. Biochem Eng J 69:113-122.
7. Elsayed MA (2014) Ultrasonic removal of pyridine from wastewater: optimization of the operating conditions. Appl Water Sci. doi:10.1007/s13201-014-0182-x.
8. Galaction AI, Kloetzer L, Turnea M, Webb C, Vlysidis A, Caşcaval D (2012) Succinic acid fermentation in a stationary-basket bioreactor with a packed bed of immobilized *Actinobacillus succinogenes* - 1. Influence of internal diffusion on substrate mass transfer and consumption rate. J Ind Microbiol Biotechnol 39:877-888.
9. Gupta VK, Jain R, Varshney S (2007) Electrochemical removal of the hazardous dye Reactofix Red 3 BFN from industrial effluents. J Colloid Interface Sci 312:292-296.
10. Harnby N, Edwards MF, Nienow AW (1997) Mixing in the Process Industries. Butterworth-Heinemann, Oxford.
11. Lataye DH, Mishra IM, Mall ID (2006) Removal of pyridine from aqueous solution by adsorption on bagasse fly ash. Ind Eng Chem Res 45:3934-3943.
12. Leyva-Ramos R, Ocampo-Pérez R, Torres-Rivera OL, Berber-Mendoza MS, Medellín-Castillo NA (2009) Kinetics of Pyridine Adsorption onto Granular Activated Carbon. Diffusion-Fundamentals.org 11:1-2.
13. Li J, Cai W, Cai J (2009) The characteristics and mechanisms of pyridine biodegradation by *Streptomyces* sp. J Hazard Mat 165:950-954.
14. Lian Q, Donghui W, Jianlong W (2010) Biodegradation of pyridine by *Paracoccus* sp. KT-5 immobilized on bamboo-based activated carbon. Bioresource Technol 101:5229-5234.
15. Mathur AK, Majumder CB, Chatterjee S, Roy P (2008) Biodegradation of pyridine by the new bacterial isolates *S. putrefaciens* and *B. sphaericus*. J Hazard Mater 157:335-343.
16. Mohan D, Sing KP, Sinha S, Gosh D (2005) Removal of pyridine derivatives from aqueous solution by activated carbons developed from agricultural waste materials. Carbon 43:1680-1693.
17. Ocampo-Pérez R, Leyva-Ramos R, Alonso-Davila P, Rivera-Utrilla J, Sanchez-Polo M (2010) Modeling adsorption rate of pyridine onto granular activated carbon. Chem Eng J 165:133-141
18. Pandoley KV, Mudliar SN, Banerjee SK, Deshmukh SC, Pandey RA (2011) Fenton oxidation: A pretreatment option for improved biological treatment of pyridine and 3-cyanopyridine plant wastewater. Chem Eng J 166:1-9.
19. Pandoley KV, Rajvaidya AS, Subbarao TV, Pandey RA (2006) Biodegradation of pyridine in a completely mixed activated sludge process. Bioresource Technol 97:1225-1236.
20. Perry RH, Chilton CH (1973) Chemical Engineers Handbook, 5th Ed. McGraw-Hill, New York.
21. Prelle MJ, Singer MF (1983) Elementary first integrals of differential equations. Trans Am Math Soc 279:215-229.
22. Rhee SK, Lee GM, Lee ST (1996) Influence of a supplementary carbon source on biodegradation of pyridine by freely suspended and immobilized *Pimelobacter* sp. Appl Microbiol Biotechnol 44:816-822.
23. Rhee SK, Lee GM, Yoon JH, Park YH, Bae HS, Lee ST (1997) Anaerobic and aerobic degradation of pyridine by a newly isolated denitrifying bacterium. Appl Environ Microbiol 63:2578-2585.
24. Sabah E, Celik MS (2002) Interaction of pyridine derivatives with sepiolite. J Colloid Interface Sci 251:33-38.
25. Sheelu G, Kavitha G, Fadnavis NW (2008) Efficient immobilization of *lecitase* in gelatin hydrogel and degumming of rice bran oil using a spinning basket bioreactor. J Am Oil Chem Soc 85:739-748 .
26. Shen J, Zhang X, Chen D, Liu X, Zhang L, Sun X, Li J, Bi H, Wang L (2014) Kinetics study of pyridine biodegradation by a novel bacterial strain, *Rhizobium* sp. NJUST18. Bioprocess Biosyst Eng 37:1185-1192.
27. Subbaramaiah V, Srivastava VC, Mall ID (2013) Catalytic wet peroxidation of pyridine bearing wastewater by cerium supported SBA-15. J Hazard Mater 248-249:355-363.
28. Williams D, Munnecke DM (1981) The production of ethanol by immobilized yeast cells. Biotechnol Bioeng 23:1813-1825.
29. Yao H, Ren Y, Deng X, Wei C (2011) Dual substrates biodegradation kinetics of m-cresol and pyridine by *Lysinibacillus cresolivorans*. J Hazard Mater 186:1136-1140.
30. Zaiat M, Rodrigues JAD, Foresti E (2000) External and internal mass transfer effects in an anaerobic fixed-bed reactor for wastewater treatment. Process Biochem 35:943-949.

II. PREPARATION OF OPTICALLY ACTIVE IBUPROFEN USING A TWO STEPS INTERCONNECTED LIPASE CATALYZED KINETIC RESOLUTION SYSTEM

Ibuprofen is one of the most important members of NSAIDs that belongs to the family of propanoic acid. Their anti-inflammatory activity resides primarily in the *S* enantiomer, more water

soluble, promoting more rapid dissolution.¹ The undesired (*R*)-profens might bring some health problems, e.g. accumulation in fatty tissues, with unknown effects.² The chirality play an important role also on the skin permeability of ibuprofen, as demonstrated.³

Biocatalysis offers a green alternative for the resolution of racemic profens, usual through kinetic resolution processes. Lipases and particularly lipase B from *Candida antarctica* (CaL-B) have been used in the resolution and preparation of chiral alcohols, carboxylic acids, esters, amides and lactones via synthesis, hydrolysis, alcoholysis, acidolysis or transesterification.⁴ Esterifications are limited by the lower activity of the biocatalysts, by the need to shift the equilibrium to the product-side (e.g. by removing the water formed in the process) and as well by long reaction times (days) and only moderate enantioselectivities and yields. Lipase-catalyzed esterification⁵ or alcoholysis⁶ could circumvent the hydrolysis disadvantages determined by the limited solubility of ibuprofen-esters in aqueous systems.

A large number of lipases and esterases have been shown to be highly enantioselective towards several profens. Not only hydrolytic approaches performed in aqueous media, but also alcoholysis and aminolysis reactions in non-conventional media were reported in the last two decades.⁷ Habibi reported recently the stereoselective hydrolysis of racemic butyl ester catalyzed by *Candida rugosa* lipase (CRL) immobilized on octyl-sepharose *via* physical adsorption, as stable catalyst, yielding the (*S*)- ibuprofen (ee \geq 95%), at low conversion (*c* <15%).⁸ The covalent attachment of the *Rhizomucor miehei* lipase on different sepharose based supports provided less active biocatalysts for the esterification of racemic ibuprofen or hydrolysis of racemic esters, even in solvents-mixtures containing ionic liquids, as demonstrated.⁹ With the aim to improve the recovery and effective reuse of the biocatalyst, important for industrial applications, Siódmiak studied the immobilization of lipases onto various activated magnetic beads, obtaining enzyme preparates with unacceptable levels of activity and enantioselectivity.¹⁰ These results are in agreement with those obtained by Marszał for the esterification of racemic ibuprofen with lipase-immobilized magnetic chitosan nanoparticles.¹¹ The solvent engineering is a general accepted strategy for fine tuning of the enzymatic activity. The solvent can modify the enzymatic activity by two means: by substrate solubilization and by conformational changes of the protein.¹² The amount of water is one of the most influential factors on the activity of lipases in organic media. The solubility of the residual water in the used solvents can significantly influence the reaction parameters. The required use of organic solvent may be an important advantage in the next isolation and purification steps of the target product.

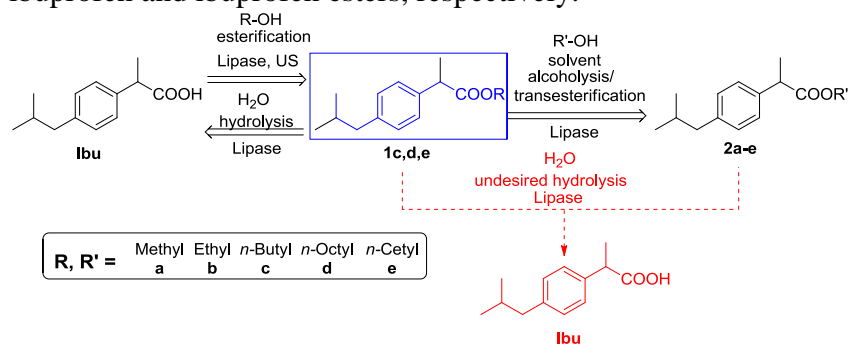
It is well known that the catalytic mechanism of lipases, acting on an acylated substrate, is undertaken through the formation of an acyl-enzyme intermediate that facilitates the nucleophilic attack. Structures such as esters of medium or long chain residues, miming the natural substrates of lipases (acylglycerols), could be a possibility to improve the enantioselectivity (substrate engineering). In addition, the esters of racemic profens with fatty alcohols are most soluble in the organic solvents. These alcohols are available at low price, environmental friendly and better tolerated by enzymes. Moreover, short-chain alcohols tend to strip the essential water from the enzyme acting as dead-end inhibitors.¹³

In the last years, a lot of papers have been published on the lipase-catalyzed biotransformation (including synthesis and/or hydrolysis) of fatty acid esters, based on the fact that they are natural like substrates,¹⁴ but not many reports on the use of long chain alcohols as nucleophile in the enzymatic esterification were found. Some authors demonstrated the low activity of lipase from *Candida rugosa* in the esterification of aliphatic acids with long chain alcohols, explained by their inhibition¹⁵ or their solvation.¹⁶ Higher enantioselectivities were observed for the reaction of substituted 2-phenoxypropionic acids with alcohols in organic solvents containing a small amount of water.¹⁷ The *n*-alkyl (C8-C14) esters of glucuronic acid have been prepared by lipase catalyzed synthesis as nonionic biodegradable, non-toxic, non-irritant for skin, odorless and tasteless surfactants.¹⁸ The esterification of lactic and glycolic acids with fatty alcohols (C8-C16) in the presence of a lipase from *Candida antarctica* was also studied and optimized.¹⁹ This synthetic

method gives nearly complete conversion to the desired ester in a relatively short time and at high volumetric productivity.

In our study the enzymatic kinetic resolution of some racemic esters of ibuprofen was performed with the aim to prepare the highly enantiomerically enriched *S* enantiomer of Ibuprofen, using the solvent and substrate engineering. In order to explore the influence of substrate structural features on the selectivity of lipase mediated kinetic resolution of racemic ibuprofen, the effect of the alcohol used as nucleophile (the length of alkyl chain) on the performance of all possible processes: esterification, alcoholysis (transesterification) and hydrolysis was studied. In the presence of a lipase as stereoselective catalyst all these routes should be stereoselective. Depend on the enzyme stereoselectivity, *R* or *S* enantiomers of the reaction counter parts could be synthesized as resumed in Scheme 2.1.

The enantioselective lipase-mediated alcoholysis *versus* lipase-catalyzed hydrolysis of different racemic esters were also studied with the aim to produce both optically pure enantiomers of ibuprofen and ibuprofen esters, respectively.



Scheme 2.1. Possible biocatalytic transformations on ibuprofen derivatives

Studying the enzymatic hydrolysis of sixteen different amides with CaL-B, Torres-Gavilán et al. have reported²⁰ the strict dependence of the hydrolysis rate on the length of the acyl residue of the substrate. The residual water content of the used solvent and/or enzyme generally allowed secondary hydrolytic reactions during alcoholysis processes (as represented in Scheme 2.1).

Furthermore, due to the water produced in the esterification reaction, at high conversion grade the favoured hydrolysis of the enantioform preferentially recognised by the lipase could occurs, with consequent final damage of the enantiomeric excess of both ester (the *R*-enantiomer, generating the *R*-acid) and unreacted acid (*S*-form).

2.1. LIPASE-CATALYZED ESTERIFICATION OF THE IBUPROFEN

First, the lipase-catalyzed esterification of racemic ibuprofen (**Ibu**) was tested under various conditions. Lipases from *Aspergillus oryzae* and *Rhizopus oryzae* were successfully used for the direct esterification of racemic phenylacetic and 2-phenyl-1-propanoic acid.²¹ Commercial lipases, such as lipases A and B from *Candida antarctica* (CaL-A and CaL-B), lipase from *Candida rugosa* (CRL, AYS Amano) and *Pseudomonas cepaciae* (PS-C II), Alcalase, lipase AK from *Pseudomonas fluorescens*, pancreatic porcine lipase (PPL) and *Mucor miehei* lipase (MML) were screened in reactions with several alcohols at room temperature under ultrasound irradiation and/or in batch process. Only the *R*-selective CaL-B was satisfactory as biocatalyst for esterification, leading to the *S* enantiomer of the acid. The presence of ultrasound media increase the reaction rate (*c* >13% after 1 h), leads to lower selectivity

It is well known that the polarity of the solvent, described by the log *P* value, influence the enzyme activity. For the enzymatic ester synthesis solvents having log *P* >4.0 are generally recommended.²² The reaction was performed in several solvents (MTBE, *n*-octane, acetonitrile, toluene, THF), which slightly improve the activity of the enzyme. Solvents such as THF or acetonitrile, more hydrophilic, strip the essential water surrounding the enzyme, leading to enzyme inactivation (~ 13% conversion after 1 h). Hydrophobic solvents such as *n*-hexane preserve the catalytic activity.

As conclusion, the kinetic resolution of Ibuprofen ester by esterification is not a suitable method for our purpose due to the low enzyme activity/long reaction time. In the presence of ultrasound an increased rate was observed, but lower enantioselectivity, even when reaction was

performed with 4 equiv. of the alcohol using an appropriate organic solvents. When different alcohols were used as nucleophile (*n*-butanol, *iso*-butanol, *n*-pentanol, *n*-octanol, *n*-hexadecanol) the enzymatic activity in neat alcohol decreased proportionally with the carbon chain length. Best results were obtained with immobilized CaL-B in MTBE as solvent (*c*= 19.6% after 1 h).

Table 2.1. Solvent (400 μ L) screening for the selective esterification of *rac*-Ibu (200 mg) with CaL-B (100 mg/mL) and *n*-butanol (4 eq) at 55°C, ultrasound, after 1h.

Entry	Solvent	<i>c</i> (%)	<i>ee</i> _{(<i>R</i>)-1c} (%)	<i>ee</i> _{(<i>S</i>)-Ibu} (%)
1	MTBE	19.6	78.4	10.7
2	acetonitrile	13.2	82.1	3.7
3	THF	12.9	83.8	28.7
4	toluene	13	75.2	12.1

2.2. LIPASE-CATALYZED HYDROLYSIS OF IBUPROFEN ESTERS

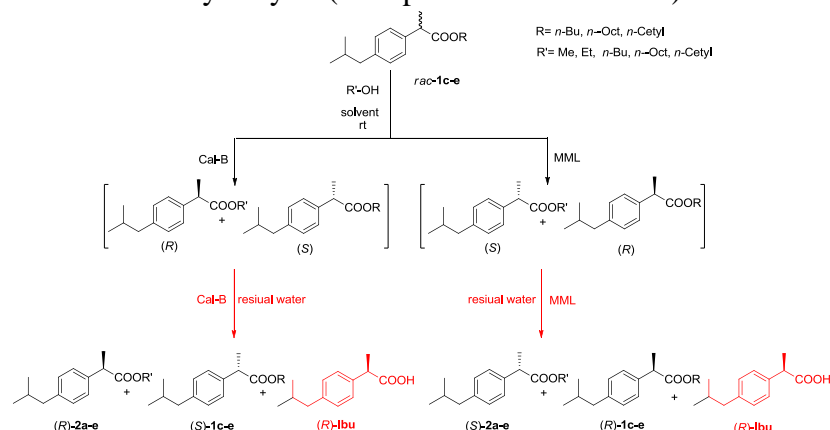
Next the hydrolysis of three bulkier racemic ibuprofen esters (*n*-butyl, *n*-octyl and *n*-cetyl, *rac*-1c-e) was performed in presence of the same lipases in the same organic solvents, but only CaL-B and MML were weakly active; the conversions were low and the enantioselectivities low to moderate. The two most efficient lipases shown opposite enantiopreferences, as illustrated in Scheme 2.2.

2.3. ENANTIOSELECTIVE ALCOHOLYSIS OF RACEMIC IBUPROFEN ESTERS

Bäckvall reported recently²³ the use of a triple-fold mutant of lipase A from *Candida antarctica* with a 30-fold enhanced activity towards profens, which displayed high enantioselectivities in the hydrolysis of ibuprofen esters with (*R*)-stereopreference, but still with rather low conversions. On the basis of this report and on our previous results for the lipase mediated *O*-acylation with fatty acids, we decided to turn our attention to the alcoholysis (transesterification) of the racemic bulkier ibuprofen esters, miming the natural substrates of lipases, with various aliphatic alcohols (Scheme 2.2).

First an extensive screening for the alcoholysis of the racemic ibuprofen *n*-octyl ester (*rac*-1d) used as model substrate (a “medium” ester) with *n*-butanol in five solvents (MTBE, *n*-octane, acetonitrile, THF, toluene) in presence of several lipases was performed at analytical scale. Most lipases (CaL-A, PPL, AK, CRL (AYS Amano), PS, and Alcalase) were inactive.

The obtained results indicated good enantioselectivity for CaL-B and MML (lipase from *Mucor miehei*), with the same opposite stereopreference found in the case of esterification/hydrolysis (as depicted in Scheme 2.2).



Scheme 2.2. The opposite enantioselectivity of CaL-B and MML in the alcoholysis of racemic ester of Ibuprofen

The presence of the *R*-enantiomer of acidic ibuprofen, formed by secondary undesired hydrolysis of esters in presence of the residual water from the enzyme preparations (shell and adsorbent), was chromatographically observed in all cases.

The inverse selectivity of some lipases was already reported in the case of lyophilized mycelia of *Aspergillus oryzae* in the resolution of (*R,S*)-Flurbiprofen.²⁴

Substrate			
Solvent			
MTBE			
ACN			
Octane			
Toluene			
THF			
Alcohol	CH ₃ OH C ₂ H ₅ OH n-C ₃ H ₇ -OH n-C ₄ H ₉ -OH	CH ₃ OH C ₂ H ₅ OH n-C ₃ H ₇ OH n-C ₄ H ₉ -OH	CH ₃ OH C ₂ H ₅ OH n-C ₃ H ₇ OH n-C ₄ H ₉ -OH

Moreover, MML was described as *S*-selective in the esterification of racemic naproxen with methanol.²⁵

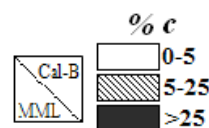


Figure 2.1. Conversions for the alcoholysis of *rac*-**1c,d,e** with CaL-B and MML in the tested solvents at room temperature, after 17 h

The process catalyzed by MML is a parallel/divergent resolution, allowing the preparation of optically enriched (*S*)-ester, which can be subsequently converts in the (*S*)-acid and of (*R*)-ester, with good conversions.

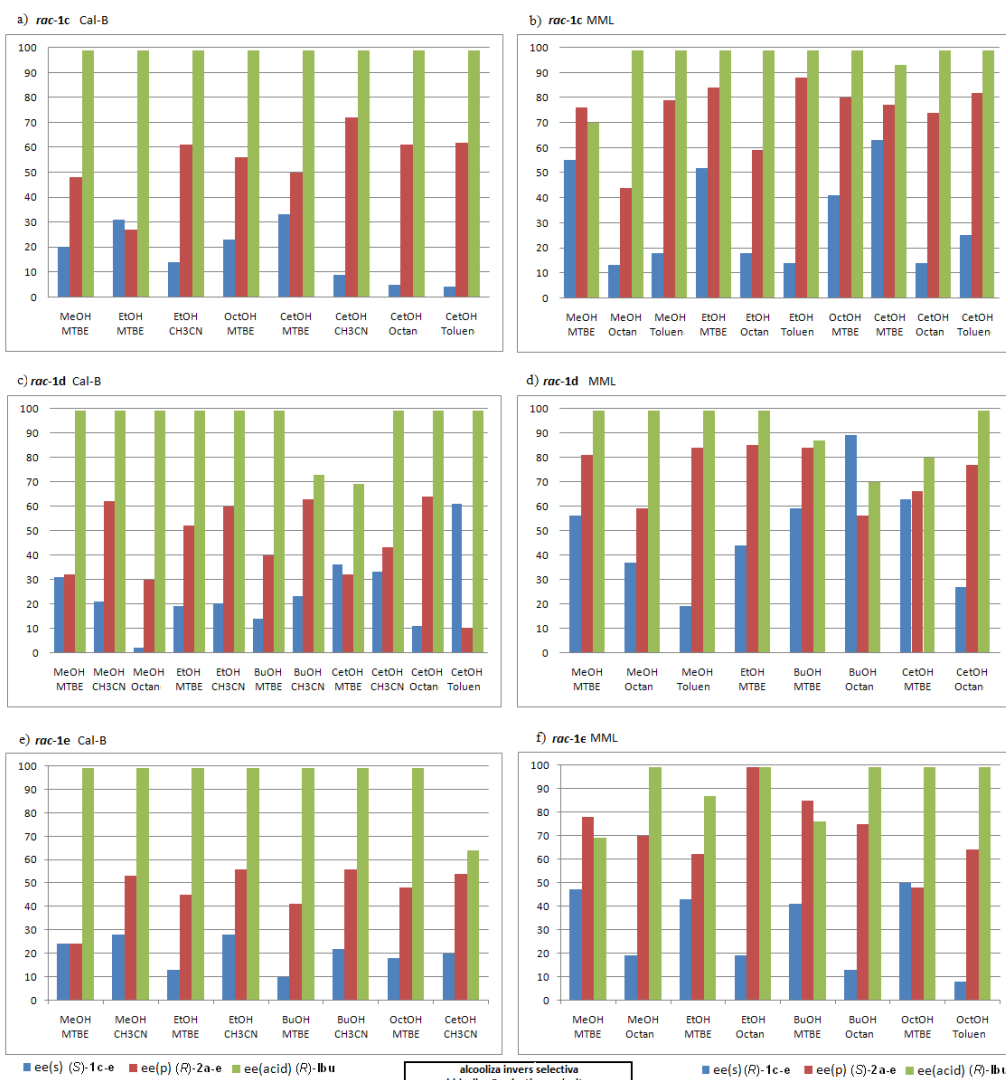


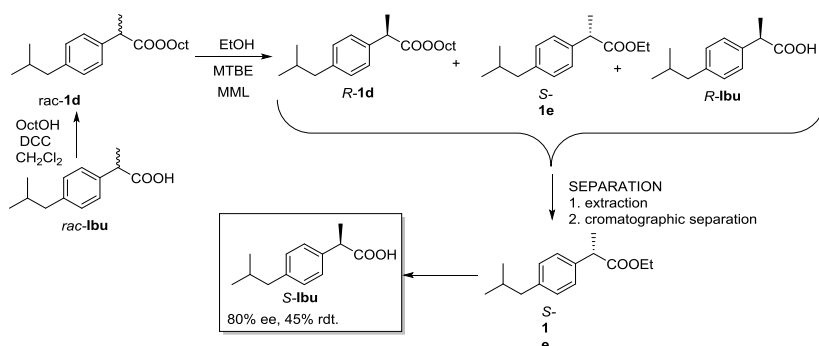
Figure 2.2. Enantiomeric excesses for the alcoholysis of the *rac*-**1c,d,e** (5 μ L) with five different alcohols (3 eq) in presence of CaL-B and MML (25mg/mL) in various solvents (500 μ L) at room temperature, after 17h

Based on these results further other nucleophiles (methanol, ethanol, *n*-butanol, *n*-octanol and *n*-cetylic alcohol) were tested for the alcoholysis of all three bulky racemic esters (*rac*-**1c-e**) in presence of these two lipases with opposite enantioselectivity in the same solvents. The obtained most relevant results are presented in Figure 2.1 (conversion) and Figure 2.2 (enantiomeric excess).

In almost all cases the optical purity of the (*R*)-ibuprofen obtained by secondary hydrolytic reactions was high, while the enantiomeric excesses of the formed (*S*)- or (*R*)-ester and of the remained (*R*)- or (*S*)-ester were moderate to good.

Concerning the obtained conversions, MTBE is the most proper solvent for the alcoholysis of all three esters with MML, with the exception of ethanolysis of the cetyl ester (**1e**) which undergoes similarly and slowly both in MTBE and *n*-octane. When CaL-B was used as catalyst, MTBE was also convenient in most of the cases. Some exceptions were observed in the case of butanolysis of octyl- and cetyl ester (**1d-e**) with CaL-B, when acetonitrile proved to be most convenient and in the case of ethanolysis of butyl ester (**1c**), when the reactions are slowly both in MTBE and acetonitrile. *n*-Octane seems to be efficient only for the octyl ester (**1d**) and MML, while THF gave in all cases very low reaction rates.

Using the optimal conditions, next the preparative scale enzymatic resolutions were realized (Scheme 2.3), obtaining both enantiomerically enriched stereoisomers of the esters. By mild hydrolysis, the *S* enantiomer of Ibuprofen, the eutomer, was obtained in an enantiomerically enriched form with good yield.



Scheme 2.3. Enzymatic synthesis of (*S*)-Ibuprofen

In conclusions, all possible enzymatic routes involving the ibuprofen esters with long chain alcohols *rac*-1 as product or substrate were studied. A selective and facile strategy to prepare both enantiomers of ibuprofen by the lipase mediated kinetic resolution of racemic *n*-octyl ester was developed.

Two enzymes with opposite enantioselectivity were tested and the influence of the chain length of alcoholic moiety on the obtained conversion and optical purity was systematically investigated. Best results were obtained for the alcoholysis of *rac*-1e with in MTBE with CaL-B or MML.

2.4. EXPERIMENTAL SECTION

The ¹H and ¹³C NMR spectra were recorded on a Bruker spectrometer operating at 300 MHz and 75 MHz, respectively, at 25°C using tetramethylsilane (TMS) as an internal standard and CDCl₃ as solvent. The enantiomeric separations were performed by HPLC using an Agilent 1200 instrument equipped with a IB (Chiral technologies) chiral columns (4.6 x 250 mm) at 25°C using 1 mL/min flow rate.

Chemical synthesis

Of the racemic compounds were performed through known methods. All compounds were characterized by spectral methods (IR, MS, NMR), see for example Figure 2.3.-2.4

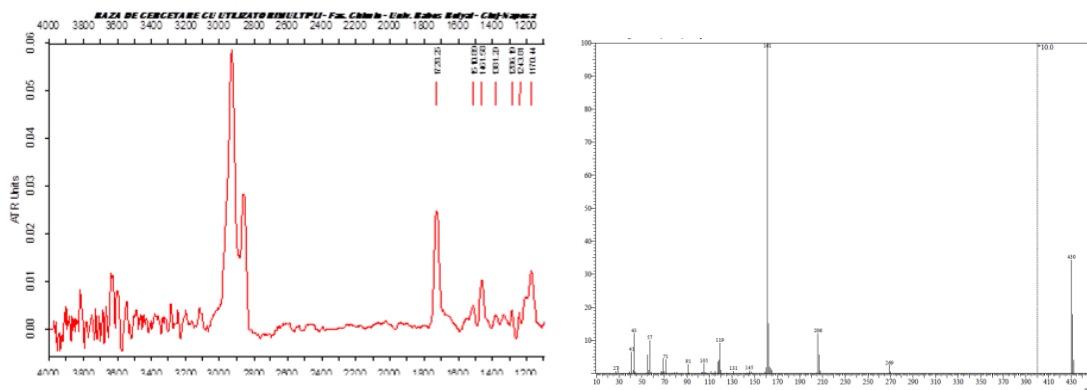


Figure 2.3. IR and MS spectra of *rac*-1c

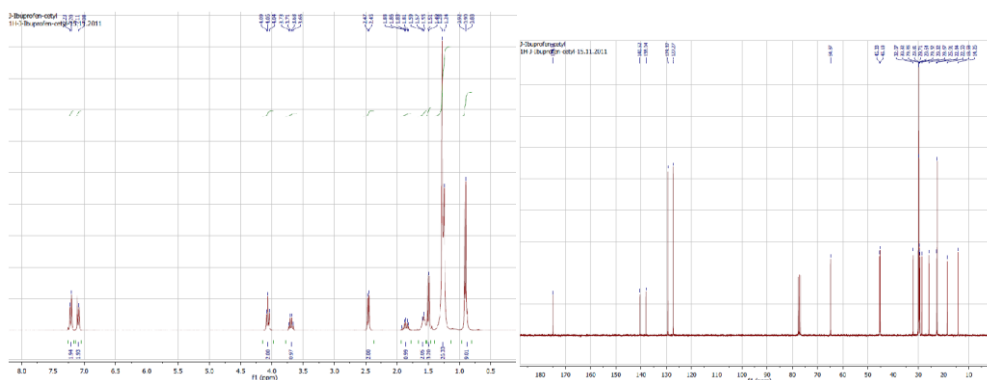


Figure 2.4. ^1H - and ^{13}C -NMR spectra of *rac*-**1c**
Analytical scale lipase mediated kinetic resolution

A. Selective esterification

One of the lipases (100 mg/mL) and an alcohol (4 eq) were added into the solution of substrate (200 mg) in an organic solvent (400 μL). The reaction mixture was performed in ultrasound irradiation at 55°C. After one hour, for the HPLC analysis, samples (50 μL) were taken from the reaction mixtures, concentrated and diluted with *n*-hexane (1 mL) before injection.

B. Selective hydrolysis

The enzyme (25 mg/mL) was added into the solution of one of the substrate *rac*-**1c,d,e** (5 μL) in an organic solvent saturated with water (500 μL). The reaction mixture was shaken (1350 rpm) at room temperature. After 17 h the reaction mixture was filtered and concentrated. 50 μL was dissolved with *n*-hexane (1 mL) and analysed by HPLC.

C. Selective alcoholysis

One of the enzyme (25 mg/mL), an alcohol (3 equiv.) and some grains of 4Å molecular sieves were added into the solution of one of the substrates *rac*-**1c,d,e** (5 μL) in the tested organic solvent (500 μL). The reaction mixture was shaken (1350 rpm) for 17 h at room temperature to reach enantiomeric composition and the conversion of the products shown in Figure 1 and 2. For the HPLC analysis, 50 μL from the reaction mixture was diluted in *n*-hexane (1 mL) before injection.

2.5. Selected literature on Part II

1. A.M. Evans, *J. Clin. Pharmacol.* **1996**, *36*, 7S-15S.
2. K. M. Williams; R. O. Day; R. D. Knihinicki; A. M. Duffield, *Acta Pharm. Toxicol.* 1986, **59**, 192–192.
3. F. Cilurzo; E. Alberti; P. Minghetti; C.G.M. Gennari; A. Casiraghi; L. Montanari, *Intern. J. of Pharm.* **2010**, *386*, 71–76.
4. a) R.D. Schmid; R.A. Verger, *Angew. Chem. Int. Edit.* **1998**, *37*, 1608–1633; b) V.B. Gotor, *Med. Chem.* **1999**, *7*, 2189–2197; c) U.T. Bornscheuer; R. J. Kazlauskas, *Hydrolases in Organic Synthesis*, Wiley–VCH, **1999**.
5. R. Morrone; N. D’Antona; D. Lambusta; G. Nicolosi: *J. Mol. Catal. B: Enzym.* **2010**, *65*, 49–51.
6. A. C. Wu; P. Y. Wang; Y. S. Lin; M. F. Kao; J. R. Chen; J. F. Ciou; S. W. Tsai: *J.Mol. Catal. B: Enzym.* **2010**, *62*, 235–241.
7. a) V. Gotor-Fernandez; E. Busto; V. Gotor., *Adv. Synth. Catal.* **2006**, *348*, 797 812; b) A.K. Prasad; M. Husain; B.K. Singh; R.K. Gupta; V.K. Manchanda; C.E. Olsen; V.S. Parmar; *Tetrahedron Lett.* **2005**, *46*, 4511–4514.
8. M. Yousefi; M. Mohammadi; Z. Habibi, *J. Mol. Catal. B: Enzymatic*, **2014**, *104*, 87-94.
9. Z. Habibi; M. Mohammadi; M. Yousefi, *Process Biochemistry* **2013**, *48*, 669-676.
10. M. P. Marszał; T. Siódmiak, *Catalysis Communications* **2012**, *24*, 80-84.
11. T. Siódmiak; M. Ziegler-Borowska; M. P. Marszał, *J. Mol. Catal. B: Enzymatic*, **2013**, *94*, 7-14.
12. W. Tsuzuki; A. Ue; A. Nagao, *Biosci. Biotechnol. Biochem.* **2003**, *67*, 1660-1666.
13. a) J.P. Chen; J.B. Wang, *Enzyme Microb. Technol.* **1997**, *20*, 615-622; b) W. Chulalaksananukul; J. S. Condoret; D. Combes, *Enzyme Microb. Technol.* **1993**, *15*, 691-698.
14. For examples, (a) Guibé-Jampel, E.; Chalecki, Z.; Bassir, M.; Gelo-Pujic, M. *Tetrahedron* 1996, *52*, 4397-4402; (b) Cesar de Jesus, P.; Rezende, M.C.; Nascimento M.D. *Tetrahedron: Asymmetry* 1995, *6*, 63-66; (c) Liaquat, M. *J. Mol. Catal. B: Enzymatic* 2011, *68*, 59-65; (d) Miyazawa, T.; Kaito, E.; Yukawa, T.; Murashima, T.; Yamada, T. *J. Mol. Catal. B: Enzymatic* 2005, *37*, 63-67; (e) Ardhaoui, M.; Falcimaigne, A.; Ognier, S.; Engasser, J.M.; Moussou, P.; Pauly, G.; Ghoul, M. *J. Biotechnol* 2004, *110*, 265-271; (f) Brem, J.; Naghi, M.; Tosa, M.I.; Boros, Z.; Poppe, L.; Irimie, F.D.; Paizs, C. *Tetrahedron: Asymmetry* 2011, *22*, 1672-1679; (g) Santaniello, E.; Casati, S.; Ciuffreda, P.; Meroni, G.; Pedretti, A.; Vistoli, G. *Tetrahedron: Asymmetry* 2009, *20*, 1833-1836; (h) Kaewprapan, K.; Wongkongkatap, J.; Panbangred, W.; Phinyocheep, P.; Marie, E.; Durand, A.; Inprakhon, P. *J. Biosci. Bioeng.* 2011, *112*(2), 124-129; (i)

- Torres-Gavilán, A.; Escalante, J.; Regla, I.; López-Munguía, A.; Castillo, E. *Tetrahedron: Asymmetry* **2007**, *18*, 2621-2624.
15. M. Holmquist; F. Haeffner; N. Orbjorn; K. Hult, *Protein Science* **1996**, *5*, 83-88.
16. Janssen, A.E.M.; Halling, P.J. *J. Am. Chem. Soc.* **1994**, *116*, 9827–9830; From, M.; Adlercreutz, P.; Mattiasson, B *Biotechnology Letters* **1997**, *19*, 315–317.
17. K. Watanabe; T. Uno; T. Koshiba; T. Okamoto; Y. Ebara; S. Ueji, *Bulletin of the Chemical Society of Japan* **2004**, *77*, 543-548.
18. C. Blecker; S. Danthine; M. Pétré; G. Lognay; B. Moreau; L.V. Elst; M. Paquot; C. Deroanne, *Journal of Colloid and Interface Science* **2008**, *321*, 154–158.
19. C. Torres; C. Otero *Enzyme and Microbial Technology* **1999**, *25*, 745-752.
20. A. Torres-Gavilán; E. Castillo; A. López-Munguía, *J. Mol. Catal. B: Enzym.* **2006**, *41*, 136–140.
21. a) R. Gandolfi; R. Gualandris; Ch. Zanchi; F. Molinari, *Tetrahedron: Asymmetry*, **2001**, *12*, 501-504; b) A. Romano; R. Gandolfi; F. Molinari; A. Converti; M. Zilli; M. Del Borghi, *Enzyme Microb. Technol.* **2005**, *36*, 432-438.
22. Lane, C., Boeren S., Vos, K., Veeger, C. *Biotechnol. Bioeng.* **1987**, *30*, 81-87
23. a) K. Engström; J. Nyhlen; A. G. Sandström; J. E. Backväll, *J. Am. Chem. Soc.* **2010**, *132*, 7038–7042; b) A. G. Sandström; K. Engström; J. Jyhlen; A. Kasrayan; J.E. Backväll, *Protein Eng., Des. Sel.* **2009**, *22*, 413–420.
24. P. Spizzo; A. Basso; C. Ebert; L. Gardossi; V. Ferrario; D. Romano; F. Molinari, *Tetrahedron* **2007**, *63*, 11005-11010.
25. R. Morrone; N. D'Antona; D. Lambusta; G. Nicolosi, *J. Mol. Catal. B: Enzymatic* **2010**, *65*, 49-51.
26. C.-S. Chen; Y. Fujimoto; G. Girdaukas; C. J. Sih, *J. Am. Chem. Soc.* **1982**, *104*, 7294-7299.

III. DISEMINAREA REZULTATELOR CERCETĂRII AFERENTE ETAPEI DIN ANUL 2016

• 2 articole publicate si 1 articol in procesare in reviste cotate ISI

1. Ramona-Mihaela Matran, Anca-Irina Galaction, Alexandra Cristina Blaga, Marius Turnea, Dan Cașcaval, Distribution of Mixing Efficiency in a Split-Cylinder Gas-Lift Bioreactor with Immobilized *Yarrowia Lipolytica* Cells Used for Olive Oil Mill Wastewater Treatment, *Chemical Engineering Communications* 2016, 203(5), 666-675.
2. Anca-Irina Galaction, Dan Cașcaval, Ramona-Mihaela Matran, Alexandra Tucaliuc, Production of Succinic Acid in Basket and Mobile Bed Bioreactors – Comparative Analysis of Substrate Mass Transfer Aspects, *Chinese J. Chem. Eng.* 2016, 24(4), 513-520.
3. Dan Cașcaval, Alexandra Cristina Blaga, Anca-Irina Galaction, Diffusional effects on anaerobic biodegradation of pyridine in a stationary basket bioreactor with immobilized *Bacillus spp.* cells, *Environmental Technology* 2016, *under review*.

• 4 participări la manifestări științifice internaționale

1. Bartha-Vári J. H., Nagy E. Z., Gal C. A., Bencze L. C., Toșa M. I., Irimie F. D., Abaházi E., Poppe L., Paizs C.: CaL-B Immobilized on Single Walled Carbon Nanotubes as Efficient Biocatalyst for the Kinetic Resolution of 1-(Hetero)aryl –Ethanol, *Systems Biocatalysis” COST Training School, Siena, Italy, 27th-30th April 2016*
2. Anca Irina Galaction, Alexandra Cristina Blaga, Lenuța Kloetzer, Dan Cașcaval, Basket bed bioreactor for immobilized biocatalysts, *International Salon Inventica* 2016, Iasi, 28 Iunie - 1 Iulie 2016 (**Medalie de Aur**)
3. GAL Cristian Andrei, Dr. 3. Bartha-Vári Judith-Hajnal, Nagy Emma-Zsófia-Aletta, Tiponut Norbert, Dr. Bencze László-Csaba, Dr. Toșa Monica Ioana, Dr. Katona Gabriel, Dr. Paizs Csaba: A CaL-B lipáz nanorészecskékre való rögzítése valamint alkalmazása optikailag tiszta aril, heteroaril szekunder alkoholok előállítására, *22nd International Conference on Chemistry*, 3-6 November 2016, Timișoara, România
4. Alexandra Cristina Blaga, Corina Paraschiva Ciobanu, Ovidiu Farcasi, Anca-Irina Galaction, Dan Cașcaval, Influence of oxygen-vectors in fumaric acid fermentation using immobilized *Rhizopus oryzae*, *3rd International Conference on Chemical Engineering*, 9-11 Noiembrie 2016, Iași, România